Decomposition of Fluoroethylene Carbonate Additive and Glue Effect of Lithium Fluoride Products for Solid Electrolyte Interphase: An Ab-Initio Study

Journal:	*Physical Chemistry Chemical Physics*
Manuscript ID	CP-ART-12-2015-007583.R1
Article Type:	Paper
Date Submitted by the Author:	03-Feb-2016

Complete List of Authors:	Okuno, Yukihiro; Fujifilm Corporation , Ushirogata, Keisuke; FUJIFILM Corporation, Research and Development Headquarters Sodeyama, Keitaro; National Institute for Materials Science, International Center for Materials Nanoarchitectonics Tateyama, Yoshitaka; National Institute for Materials Science, International Center for Materials Nanoarchitectonics

PCCP

ARTICLE

Decomposition of Fluoroethylene Carbonate Additive and Glue Effect of Lithium Fluoride Products for Solid Electrolyte Interphase: An Ab-Initio Study

Received 00th January 20xx,
Accepted 00th January 20xx

DOI: 10.1039/x0xx00000x

www.rsc.org/

Yukihiro Okuno,*[ab] Keisuke Ushirogata[ab], Keitaro Sodeyama[bc] and Yoshitaka Tateyama*[bd]

Additives in the electrolyte solution of lithium-ion batteries (LIBs) have a large impact on the performance of the solid electrolyte interphase (SEI) that forms on the anode and is a key to the stability and durability of LIBs. We theoretically investigated effects of fluoroethylene carbonate (FEC), a representative additive, that has recently attracted considerable attention for the enhancement of cycling stability of silicon electrodes and the improvement of reversibility of sodium-ion batteries. First, we intensively examined the reductive decompositions by ring-opening, hydrogen fluoride (HF) elimination to form vinylene carbonate (VC) additive and intermolecular chemical reactions of FEC in ethylene carbonate (EC) electrolyte, by using density functional theory (DFT) based molecular dynamics and the blue-moon ensemble technique for the free energy profile. The results show that the most plausible product of the FEC reductive decomposition is lithium fluoride (LiF), and that the reactivity of FEC to anion radicals is found inert compared to the VC additive. We also investigated the effects of the generated LiF on the SEI by using two model systems; (1) LiF molecules distributed in a model aggregate of organic SEI film components (SFCs) and (2) a LiF aggregate interfaced with SFC aggregate. DFT calculations of the former system show that F atoms form strong bindings with the Li atoms of multiple organic SFC molecules and play as a joint connecting them. In the latter interface system, the LiF aggregate adsorbs the organic SFCs through the F-Li bindings. These results suggest that LiF moieties play a glue role for the organic SFC within the SEI film. We also examined the interface structure between a LiF aggregate and a lithiated silicon anode, and found that they are strongly bound. This strong binding is likely to be related to the effectiveness of FEC additive in the electrolyte for the silicon anode.

1 Introduction

Because of their high-energy density characteristics, lithium-ion batteries (LIBs) have drawn considerable attention for use in large power sources like those used in electric vehicles and energy storage systems[1.,2.]. To make such uses practical, a higher degree of safety, a longer cycle life as well as higher voltage and capacity are crucial targets. An important key in LIB stability and durability is the solid electrolyte interphase (SEI) that is formed at the interface between the negative electrode and the electrolyte[1.-40.]. It is generally accepted that molecules in the electrolyte solution reductively decompose to form various SEI film components (SFCs), which include organic oligomers such as dilithium ethylene dicarbonate (Li_2EDC) and inorganic moieties such as Li_2CO_3, and LiF, at the first charging[5.].

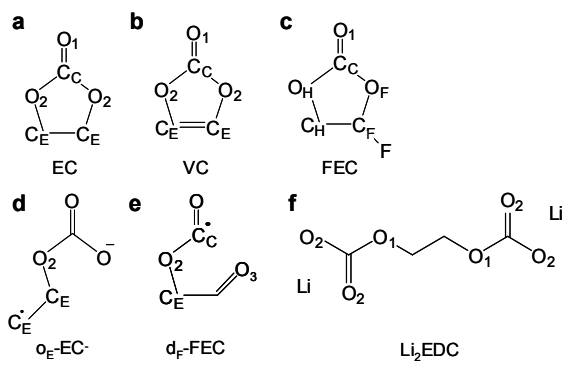

Figure 1. Molecular structures of (a) ethylene carbonate (EC), (b) vinylene carbonate (VC), and (c) fluoroethylene carbonate (FEC) with the atomic labels used throughout this paper, along with structures of (d) o_E-EC$^-$ is a anion radical generated by one-electron reductive decomposition of EC, (e) d_F-FEC, a neutral radical produced by FEC decomposition after F^- ion release, and (f) dilithium ethylene dicarbonate (Li_2EDC), a candidate SFC generated from EC electrolytes. On FEC molecules, we refer C_C-O_H and C_C-O_F (C_H-O_H and C_F-O_F) bonds as 'shoulder' (waist) bonds of FEC in the text.

[a.] Research and Development Headquarters, FUJIFILM Corporation, 210 Nakanuma, Minamiashigara, Kanagawa 250-0193, Japan.
E-mail: yukihiro.okuno@fujifilm.com
[b.] International Center for Materials Nanoarchitectonics (MANA), National Institute for Materials Science (NIMS), 1-1 Namiki, Tsukuba, Ibaraki 305-0044, Japan.
E-mail:TATEYAMA.Yoshitaka@nims.go.jp
[c.] PRESTO, Japan Science and Technology Agency (JST), 4-1-8 Honcho, Kawaguchi, Saitama 333-0012, Japan
[d.] Elements Strategy Initiative for Catalysts & Batteries, Kyoto University, Goryo-Ohara, Nishikyo-ku, Kyoto 615-8245, Japan.
Electronic Supplementary Information (ESI) available.
See DOI: 10.1039/x0xx00000x

The SFCs precipitate on the electrode surface to form a SEI film with a thickness of several tens of nanometers[6.].

The electrolyte additives are often used to improve the SEI quality[14.]. In fact, the use of small amounts of additives in the electrolyte has been found to drastically improve the stable cycle efficiency, capacity retention, and thermal stability of the anode[10.-14.]. Fluoroethylene carbonate (FEC) (Fig. 1 (c)) is one of the commonly used additives[41.-51.].Recently, FEC has attracted attention because it efficiently enhances the cycling behaviors of silicon electrodes[41.-46.], and improves the reversibility of sodium-ion batteries[48.]. Experimental studies of the SEI structure formed in the presence of FEC have reported discrepant results with regard to, for example, the existence of polycarbonate components[42.-44.,46.] and the thickness of the SEI film. In addition, the mechanism by which FEC exerts its effect is still under debate. One of the famous mechanisms proposed for the FEC effect is the elimination of hydrogen fluoride (HF) from the FEC molecule to form vinylene carbonate (VC) derivatives[14.,49.], although this mechanism has not been well established. Therefore, the nature of SEI formed by FEC decomposition, the chemical reactions involved, and the resultant reaction intermediates remain to be elucidated.

Theoretical and computational studies are powerful means for examining behavior and reaction of molecules near electrode surfaces on the atomic scale. The reaction mechanisms of typical solvents such as ethylene carbonate (EC) and typical additives like VC were extensively studied a decade ago by means of cluster boundary condition (CBC) density functional theory (DFT)[32.-34.]. Recently, more sophisticated DFT-based molecular dynamics (DFT-MD) methods have been employed to study their reaction mechanisms near the electrode, even though these methods are computationally demanding[35.-40.]. Concerning the FEC additive, there are DFT-MD studies that examined the one- and two-electron reductive decomposition reactions of FEC on silicon and lithiated silicon anode[52.-54.]. Their results suggest a plausible FEC^- decomposition path by comparing with the free energies of reaction intermediates estimated by means of CBC-DFT methods[52.,53.]. The common aspects of these studies indicate that a F^- ion is produced by a reduction process with a small[52.,54.] or moderate[53.] energy barrier and that the F^- ion forms LiF moieties in the SEI, which is consistent with some experimental observations in the presence of FEC[42.-47.]. Although those studies provided many aspects, they mainly discussed the observation of spontaneous processes of one FEC molecule by means of a DFT-MD method or a static calculation of the free energies of reaction intermediates by CBC-DFT method. A complete understanding of the reaction mechanisms, however, requires information about the kinetics of various processes of decomposition and binding reactions, including the solvation dynamics and temperature effect. Furthermore, the relationship between the products of FEC decomposition (e.g., LiF) and their effects on the LIB performance is unclear. Conventionally, it is thought that inorganic SFCs such as LiF suppress Li ion transport inside and are regarded to be harmful compared to organic SFCs. If the main role of FEC in LIB is the production of LiF, an inorganic SFC, then the mechanism by which LiF improves LIB performance is a crucial subject to be examined.

In this study, we examined the reductive decomposition of FEC additive and the effect of LiF, a probable product of that decomposition, on SEI formation. First, we investigated possible one- and two-electron reductive decomposition pathways by means of a DFT-MD method, and blue-moon ensemble technique to evaluate thermodynamically spontaneous behaviors as well as activation free energies. On the basis of the results, we propose the most plausible reaction pathway and products. We also examined the possibility of HF elimination from FEC to form VC, which was suggested by previous researches[14.,49.], and compared the reactivity of neutral FEC and VC to the corresponding radical molecules, as we studied in our previous studies[39.,40.]. Second, we investigated the role of LiF in the organic SFC by means of DFT-MD calculations, using two model systems; (1) LiF molecules distributed in an organic SFCs aggregate and (2) a LiF aggregate interfaced with organic SFC aggregates. We also compared the properties of the interface between LiF aggregate and two model electrodes, pristine graphite and lithiated silicon, because FEC has shown to be to effectively enhance the cycling behaviors of silicon electrodes[41.-46.]. Then, the interface states are discussed in terms of the possible origins of the improvement of LIB performance in the presence of FEC, such as a decrease in irreversible capacity loss[42.] .

2 Calculations

2.1 DFT Molecular Dynamics

To investigate the reductive decomposition of FEC, we carried out DFT-MD calculations using supercells consisting of 31 EC molecules and one FEC molecule (FEC/EC system) with or without one Li atom. A cubic box with a dimension of 15.24 Å was used as the supercell to reproduce an EC density of 1.32 g/cm^3.[29,30] To model a mixture of LiF in an aggregate of Li_2EDC, the most representative EC-derived SFC, we used 17.95 Å cubic supercell where 40 Li_2EDC molecules were involved. The size of the supercell for the Li_2EDC condensed phase was determined on the basis of the reported density of Li_2EDC, 1.86 g/cm^3, which was obtained with classical MD calculations under ambient conditions[24.-26.]. For adsorption of a LiF aggregate on a Li_2EDC aggregate in an EC electrolyte, we used a supercell consisting of LiF amorphous structure aggregate ($Li_{64}F_{64}$), 16 Li_2EDC molecules, and an electrolyte composed of 72 EC molecules. The initial structures of all the components were taken from equilibrium trajectories of classical MD or DFT-MD simulations. In addition, we included two model anodes, H-capped graphite and lithiated silicon. The H-capped graphite anode consisted of four graphite sheets where each sheet has 5 × 6 hexagonal rings, and was modeled as $C_{288}H_{46}Li_{12}$. Note that we selected the H-capped graphite because we focus on the reductive environment in the charging process where H-capping is more probable than the other oxidized ones such as OH-capping. The lithiated silicon anode was modeled as a crystalline LiSi alloy composed of $Li_{64}Si_{64}$. The periodic boundary condition was adopted to deal with the liquid state at constant density. Typical supercells we used in the DFT-MD calculations are shown in Figure 2.

We carried out DFT-MD simulations in the framework of Car-Parrinello dynamics[55.], by using CPMD code[56.]. A fictitious electronic mass of 600 a.u. and a time step of 5 a.u. (0.12 fs) were chosen. The system temperature was controlled with a Nosé thermostat[57.,58.] at a target temperature of 353 K. After equilibration statistical averages were computed from trajectories of at least 5 ps in length. The electronic wave function was quenched to the Born-Oppenheimer surface about every 1 ps in order to maintain adiabaticity. The free energy profiles of the decomposition process were evaluated by means of blue-moon ensemble technique[59.]. We checked the sampling convergence at every point of mechanical constraint in the blue-moon ensemble. We used the PBE[60.,61.] exchange correlation functional. Stefan Goedecker's norm-conserving pseudopotential[62.-64] for C, H, O, Li ,F and Si were used.

2.2 CBC-DFT Analysis.

We used CBC-DFT methods as implemented in Gaussian 09[66.] to estimate the electron affinities of EC, VC, and FEC molecules. To complement the DFT-MD results, we also used CBC-DFT method to explore the reductive decomposition pathways of FEC molecules. The exchange and correlation functionals used were B3LYP[65] and PBE[60.,61.] with the 6-311++G(d,p) basis set and the geometries were fully optimized. In the analyses, the solvent effect was dealt with by means of the polarizable continuum model (PCM) method with parameters for an EC bulk solution (dielectric constant ε = 89.78).

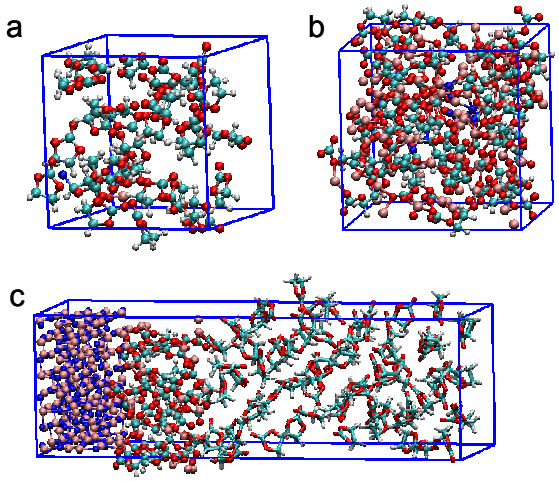

Figure 2 Supercell structures of (a) 31 EC molecules and one FEC additive (FEC/EC system), (b) 40 Li_2EDC molecule aggregate with 10 LiF molecules, (c) 16 Li_2EDC molecules aggregate on LiF amorphous aggregate ($Li_{64}F_{64}$) with 72 EC molecules. The sizes of the supercells are cubic boxes of 15.24 and 17.95 Å for (a) and (b), respectively, and rectangular box of 16.43 × 50.75 × 16.43 Å for (c).

3 Reductive decomposition of FEC

3.1 Li^+ solvation structure

We first examined the solvation shell structure of the Li^+ ion in the FEC/EC system before reduction. As in the case of the VC/EC system[39.], the most stable structure was the tetrahedral coordination of 4 EC solvents via the oxygen atoms in their carbonate groups, labeled as Li-4EC. We also found that the coordination with three EC and one FEC molecules (labeled as Li-3EC1FEC) has higher average energy of the equilibrium trajectory than the Li-4EC solvation by 5.9 kcal/mol. Furthermore, in the DFT-MD simulation of the Li-3EC1FEC system, we observed exchange from FEC to EC in the first solvation shell, resulting in the Li-4EC structure in the end. The snapshots of DFT-MD trajectories on Li-4EC and Li-3EC1FEC solvation structures are shown in Supporting Information.

In the FEC case, coordination to the Li^+ ion via the F moiety may also be possible. However, the DFT-MD simulations starting from this solvation structure showed spontaneous separation between FEC and the Li^+ ion, indicating that the fluorine atom of the neutral FEC molecule is not reactive to the Li^+ ion. Consequently, there was no preference for coordination of the FEC additive to the Li^+ ion in the EC solvent[28.]. To examine the reduction tendency, we evaluated the electron affinities (EA) of FEC and EC molecules coordinating and uncoordinating to a Li^+ ion by means of CBC-DFT calculations at the PCM-B3LYP and PCM-PBE /aug-cc-pVTZ levels (Table 1). For comparison, we examined the VC cases as well. Comparing between the two functionsl, B3LYP and PBE, we confirmed that the functional dependence is really small. As discussed in our previous study[39], the EA difference between EC and VC, 0.28-0.29 eV, is consistent with the energy difference of the reductive peak positions in cyclic voltammetry[17] for EC and VC molecules (0.3 eV). Therefore, EA is a good measure for the reduction tendency.

Table 1. Calculated electron affinity (in eV) of EC, VC and FEC molecules, and those coordinating to a Li^+ ion in the EC solution (labelled as EC/VC/FEC with Li^+). We used CBC-DFT calculations at the PCM-B3LYP and PCM-PBE /aug-cc-pVTZ levels. The Δ SCF method, which takes the total energy difference between the intact neutral molecule and monoanion molecule, was used for the evalulation of the electron affinity.

	PCM-B3LYP	PCM-PBE
EC	1.40	1.40
EC with Li^+	1.76	1.75
VC	1.69	1.68
VC with Li^+	2.04	2.00
FEC	1.74	1.74
FEC with Li^+	2.10	2.06

In Table.1, we found that the EA of FEC (1.74 eV) is almost the same as that of EC coordinating to Li^+ ion (1.75-1.76 eV). Based on the stability of solvation structure described above, this indicates that the FEC additive will not always be reduced prior to reduction of the EC solvent, and that some EC anion radicals may coexist with the reduced FEC at the initial stage of the electrolyte reduction, as in the case of the VC additive which also has no preference of coordination to the Li^+ ion in the EC solvent[39]. The EA difference between FEC and EC with Li+ is ca. 0.01-0.02 eV, smaller than that in the VC additive case (0.07 eV). Thus, the amount of EC anion radicals is expected to be lower in the FEC addtive case than VC, because FEC is likely to be reduced to the same extent of EC coordinating to Li^+ ion at the initial stage.

3.2 One-electron reductive decomposition of FEC

Next we investigated possible one-electron reductive decomposition of the FEC additive in the EC solvent. During the DFT-MD simulations, we checked whether the excess electron was localized on the FEC molecule. We then carried out constrained MD calculations in the framework of the blue-moon ensemble technique for the decomposition reaction barriers. We first evaluated the one-electron (1e) reductive decomposition of FEC via breaking of one of the "shoulder" bond of the molecule, that is, the C_C-O_H or C_C-O_F bond (Fig.1 (c)). The constraint, ξ_1, was set to the bond length of C_C-O_H or C_C-O_F. For the C_C-O_F bond, we examined the cases of FEC molecule with and without coordination to the Li^+ ion. For the coordinating FEC molecule, we considered the case where the O_1 atom coordinates to the Li^+ ion and the case in which the O_F oxygen coordinates.

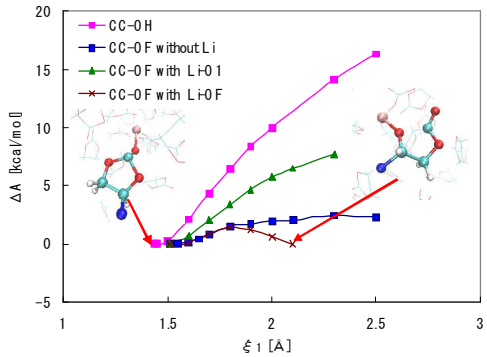

Figure 3 Free energy profiles, ΔA, for one-electron reductive decomposition of FEC^- along the mechanical constraint ξ_1 of the C_C-O_H (pink) and C_C-O_F bonds (blue, green and brown). For the C_C-O_F bond, we considered three cases; one in which the FEC^- anion does not coordinate to a Li^+ ion (blue), and two in which FEC^- coordinates to a Li^+ ion, either through the oxygen O_1 (Li-O_1: green) or O_F (Li-O_F: brown), respectively.

Fig. 3 shows the resultant free energy profiles with respect to ξ_1. We took the free energies associated with the distances of 1.43 Å (equilibrium bond distance of C_C-O_H in the FEC^- anion) and 1.51 Å (equilibrium bond distance of C_C-O_F in the FEC^- anion) as the zero reference for the C_C-O_H and C_C-O_F bond-breaking, respectively. In Fig. 3, we can find the free energy profiles of C_C-O_H and C_C-O_F bond-breaking in the absence of a Li^+ ion increased monotonically with increase of the constraint. Therefore, it seems unfavorable to break the "shoulder" bonds of FEC, C_C-O_H/C_C-O_F, by one-electron reduction. However, the free energy associated with C_C-O_F bond cleavage was very low (ca. 2.5 kcal/mol) at a bond length of 2.5 Å in the absence of a Li^+ ion (Fig. 3, blue). The presence of a Li^+ ion coordinated by the O_F oxygen of FEC stabilized the free energy profile for C_C-O_F bond cleavage and generated the LiF molecule in the end with the C_F-F bond cleavage. After the F^- ion release, the structure of FEC becomes d_F-FEC, as shown in Fig.1 (e), a neutral radical with cleavage of C_C-O_F bond. The activation free energy associated with LiF generation was estimated to be very small (ca. 1.8 kcal/mol). Thus, the FEC^- anion tends to form a LiF molecule when the Li^+ ion was close to the F atom. In contrast, when FEC^- coordinated to a Li^+ ion via O_1, the free energy needed for C_C-O_F bond cleavage increased to 7.7kcal/mol at a bond length of 2.3 Å.

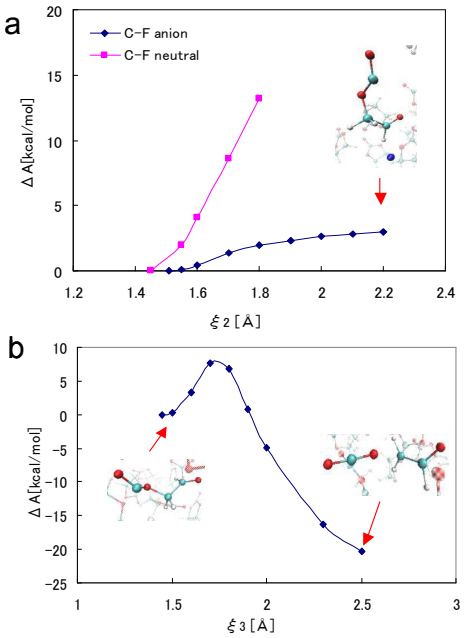

Figure 4 (a) Free energy profiles, ΔA, for one-electron reductive decomposition of neutral FEC and the FEC^- anion along the mechanical constraint ξ_2 of their C_F-F bonds. (b) Free energy profile for decomposition of the d_F-FEC neutral radical into CO_2 and CH_2COH along the mechanical constraint ξ_3 of C_E-O_2 bond distance in d_F-FEC.

The tendency of FEC^- anion to form LiF when the Li^+ ion is in an appropriate location was observed by DFT-MD calculations performed with the initial condition that the Li^+ ion was located near the F atom of the FEC^- anion. The results of three independent DFT-MD runs with these initial conditions showed spontaneous generation of LiF within 0.1ps. LiF generation from FEC^- proceeded with almost no activation barrier. These results are consistent with experimental results indicating that the amount of LiF moieties increases in the presence of added FEC[41.,45.]. With the same initial configurations, we also carried out the DFT-MD calculations with neutral FEC and observed spontaneous separation of FEC from the Li^+ ion. Therefore, the reactivity of the F atom toward the Li^+ ion was due to the reduction of FEC molecule.

Considering this pathway of LiF generation, we investigated cleavage of the C_F-F bond of FEC by 1e reduction reaction. We evaluated the free energy profile for cleavage of the C_F-F bond of FEC^- and compared it with the profile of neutral FEC (Fig. 4 (a)). In Fig. 4 (a), we set the C_F-F bond distance as the mechanical constraint ξ_2 for both neutral and anion cases. The zero-energy reference values were set to the free energies associated with the C_F-F bond lengths of 1.45 Å (the equilibrium C_F-F bond length of neutral FEC) and 1.51 Å (the equilibrium C_F-F bond length of the FEC^- anion) for the neutral FEC and the FEC^- anion cases, respectively. In the case of neutral FEC, it was observed that the FEC quickly decomposed to CO_2 and C_2OFH_3 moiety with elongation of C_F-F bond. As expected, this pathway requires a substantial activation free energy. For the FEC^- anion case, Fig. 4 (a) shows that the free energy associated with the C_F-F bond breaking was a small value of about 3kcal/mol, estimated at the C_F-F bond distance 2.2 Å. A F^- ion was released by C_F-F bond cleavage, producing a d_F-FEC neutral radical (Fig.1 (e)).

As the F^- ion was released from the FEC^- anion, the C_C-O_F bond was broken concertedly due to the driving force to form the double bond on an oxygen atom (O_3 of Fig.1 (e)), as in the case of C_C-O_F bond cleavage with LiF molecule generation. Therefore, the C_F-F and C_C-O_F bonds cooperate with each other regarding their bond breakings. The small activation free energy for C_F-F bond cleavage and connection of this bond to the C_C-O_F bond can be explained by analysis of molecular orbitals (see Supporting Information (ESI) for details). The HOMO-2 orbital of the FEC^- anion undergoing C_C-O_F bond breaking has some characteristics of σ^* type orbital of C_F-F. This orbital induces the C_F-F bond cleavage, resulting in formation of the C_F=O_F double-bond.

To investigate further decomposition of the d_F-FEC neutral radical, we calculated the free energy profile of its decomposition into CO_2 and CH_2COH neutral radical as shown in Fig. 4 (b). We set the C_E-O_2 bond distance as the mechanical constraint ξ_3 in d_F-FEC (Fig.1(e)). The activation energy was estimated to be about 7.7 kcal/mol, and the reaction free energy was lower than -20 kcal/mol. This activation energy, which is not negligible, shows that the radical d_F-FEC does not decompose immediately and remains in the electrolyte for a while. If d_F-FEC does not react with the species in the electrolyte or if it is not further reduced, it will decompose and generate CO_2 gas. Therefore, if the 1e reduction of FEC predominates in the electrolyte, CO_2 gas will be detected.

On the "waist" bonds of FEC, we also analyzed the free energy profile for cleavage of C_H-O_H and C_F-O_F bonds in the FEC^- anion. When we set the mechanical constraint as only the C_H-O_H or only the C_F-O_F bond, we observed strong hysteresis of the free energy profile. This indicates that a single C_H-O_H or C_F-O_F bond was not an appropriate reaction coordinate. For example, when we set the C_F-O_F bond length as mechanical constraint and elongated the C_F-O_F bond, the C_H-O_H bond promptly broke. For that reason, we set the sum of the bond distances of C_H-O_H and C_F-O_F as the mechanical constraint. Alongξ_4 (=C_H-O_H+C_F-O_F) elongated, we observed C_H-O_H bond cleavage predominantly. Fig. 5 indicates that cleavage of the C_H-O_H bond in the FEC^- anion was highly exothermic, and the activation free energy was 8.7 kcal/mol. In fact, the average energies of the equilibrium DFT-MD trajectories were consistent with this free energy profile: the products of cleavage of the C_H-O_H and C_F-O_F bonds of the FEC^- anion were 29.5 and 16.6 kcal/mol lower in average energy, respectively, than the ring-closing FEC^- anion. Therefore, those cleavages are thermodynamically favorable. On the other hand, the activation free energy was higher than that of LiF generation with C_C-O_F bond breaking. Furthermore, we observed that, in four of the five DFT-MD runts starting from different initial states, electron transfer from FEC^- to an EC molecule occurred within 5 ps during the dynamics at the transient state where ξ_4=3.1 Å. In fact, CBC-DFT calculations showed that electron transfer from FEC^- to EC was energetically favorable (details are provided in ESI). Thus, the electron transfer to EC can be expected to occur prior to reductive C_H-O_H bond cleavage, and the "waist" bond cleavage of the FEC^- anion cannot be the predominant process in practice.

In summary, one-electron reductive decomposition of FEC mainly takes place through cleavage of the "shoulder" bond, C_C-O_F, leading to LiF generation.

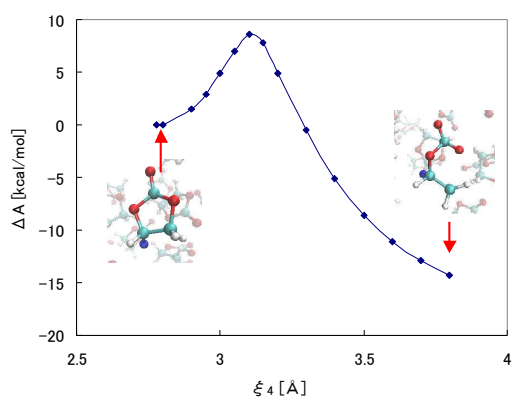

Figure 5 Free energy profile, ΔA, for cleavage of the "waist" bonds of the FEC^- anion. The mechanical constraint, ξ_4 , was set as the sum of the lengths of the 'waist ' bonds C_H-O_H and C_F-O_F bonds.

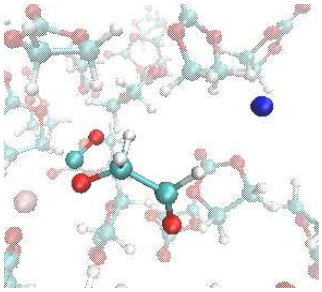

Figure 6 Snapshot of the equilibrium product state for two-electron reductive decomposition of FEC.

3.3 Two-electron reductive decomposition of FEC

We next examined the 2e reductive decomposition of FEC. Recent DFT-MD studies of FEC in a system with a Si anode treated multi-electron reduction by using a highly lithiated electrode surface[54.].

These multiple electron reductions seem to predominate during the initial stage of SEI formation, where the electron transfer from the electrode to the electrolyte is smooth enough. We added an excess electron to three randomly chosen configurations in the trajectory of the 1e reduced FEC coordinating to a Li^+ ion via its carbonyl oxygen (O_1) and then carried out DFT-MD sampling.As shown in Fig.6, we observed the FEC^{2-} decomposed into F^- + CO + $C_2H_3O_2^-$ in the two cases and the other one shows the decomposition into F^-+$C_3H_3O_3^-$ within 0.2 ps. All the reactions started with cleavage of the C_C-O_F bond. The production of F^- and CO from an FEC molecule is consistent to the DFT-MD results reported by Leung et. al[52..] Therefore, the F^- ion is also released from FEC by 2e reduction, and likely reacts with Li^+ ion that exists in the electrolyte abundantly. If 2e-reduction of FEC predominates in the electrolyte, CO gas will be detected as a result of the decomposition of FEC.

3.4 HF elimination of FEC

Here, we examined elimination of HF from the FEC molecule. As described in the introduction, it has been proposed that the predominant mechanism of FEC reaction in the electrolyte is the HF elimination to form VC[14,49.]. Because cleavage of the C-F bond in neutral FEC is difficult, as shown in Fig.4, HF elimination from neutral FEC is implausible. Therefore, we calculated the free energy profile for the HF elimination from FEC^- anion, using the distance between H and F atoms as the mechanical constraint, ξ_5, and setting the zero reference free energy as the free energy associated with the distance of 2.3 Å, which is the average value of that of FEC^- anion. As the mechanical constraint decreased from the 2.3 to 1.1 Å (Fig. 7), the F atom dissociated from the FEC^- anion first, and approached the H atom. Then, H atom was detached from the FEC^- and bonded to the F atom. In concert with the dissociation of the F atom, the C_C-O_F bond was cleaved, and the FEC^- anion was transformed to a ring-opened structure.

This is just a concerted reaction between C_F-F and C_C-O_F bond as seen in the case of the C_F-F bond cleavage in FEC^-. Finally, the H-F distance decreased to that of a HF molecule (ca. 1.0 Å), and the reminder of the FEC^- anion after HF elimination further decomposed to CO and $C_2H_2O_2^-$.

Figure 7 Free energy profile, ΔA, for the elimination of HF from the FEC^- anion along the mechanical constraint ξ_5 of the H-F distance as indicated.

These species correspond to the products of VC decomposition by one-electron reduction (CO and d_{CO}-VC^- in our previous study[39.]). Therefore, the HF elimination of FEC^- does not lead to the formation of VC molecule. On the free energy profile depicted in Fig. 7, there are two peaks along the mechanical constraint ξ_5, the H-F distance; the peak around 1.9 Å corresponds to dissociation of the F atom from the FEC^- anion, and the H atom detachment occurred around the 1.3 Å peak. The activation free energy associated with HF elimination was estimated as 5.1 kcal/mol. The average energy for

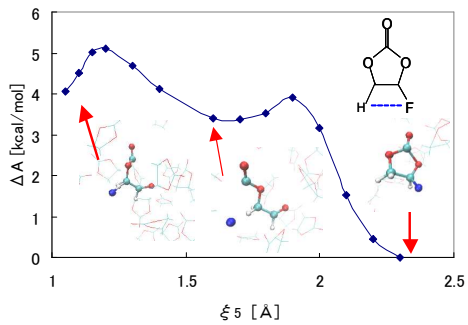

decomposition of FEC^- into HF + CO + d_{CO}-VC^- is about -3.0 kcal/mol; that is, the reaction is exothermic. Therefore, HF elimination from FEC^- may occur in EC solvent, but our calculations indicate that the formation of VC from FEC via release of HF and subsequent VC polymerization to form polycarbonates as previously suggested[14.,49.] is not feasible in the liquid electrolyte in the absence of surface. Note that Martinez et al.[54.] observed a reaction path in which reduced FEC releases F^- ion, which bonds to hydrogen originally adsorbed on a Si anode surface. The resultant product is a ring-opened (via the C_C-O_2 bond) VC^{2-} anion on the lithiated Si anode, according to their DFT-MD simulations. However, this reaction is based on a three-electron reduction, in contrast to our 1e reduction treatment. Besides, the ring-opened VC with the C_C-O_2 bond cleavage is unstable and likely to further decompose to CO and rather inert d_{CO}-VC as we have shown previously[39.]. Therefore, it is uncertain whether a polymerized structure for SFC is obtained as the final product in this process.

In consequence, the present results indicate that VC formation from FEC via HF elimination is not plausible due to the ring cleavage of FEC during the reaction.

3.5 Reactivity of FEC and its decomposition products

We have shown that the decomposition of one- and two-electron reductive decomposition reactions of FEC in detail and the essence of the FEC additive is easy release of F^- ion in the reduced states and the generation of LiF with almost no activation energy as long as a Li^+ ion exists around the F atom. Here, we investigated the reactivity of neutral FEC and the d_F-FEC neutral radical (Fig. 1(e)), which is the resultant moiety after the release of F^- ion from FEC^-, toward the o_E-EC^- anion radical (Fig. 1(d)) as a representative example. We chose C_F, C_H,

and C_C carbon atoms as the sites in the FEC molecule that are attacked by the anion radical, and we determined the reactive site of d_F-FEC by investigating its spin-localized site (C_C). For the reaction of neutral FEC on atoms C_F and C_H, we estimated the reaction barrier by carrying out blue-moon ensemble calculations with two types of mechanical constraints; distances from $C_E^{\cdot}$ of o_E-EC$^-$ to C_F and C_H in FEC, respectively. We also estimated the free energy profile of the reaction between o_E-EC$^-$ and intact VC for comparison. The reaction processes we investigated are summarized in Scheme1. The calculated free energy profiles are shown in Fig. 8.

The reaction free energies are about 17.5 and 9.0 kcal/mol for the attack o_E-EC$^-$ anion radical at the C_H and C_F atoms of FEC, respectively. In particular, reduction on the fluoroethylene side (between $C_E^{\cdot}$ and C_F) was highly exothermic. On the other hand, the activation free energies were 22 and 26 kcal/mol for the $C_E^{\cdot}$-C_H and $C_E^{\cdot}$-C_F processes, respectively.

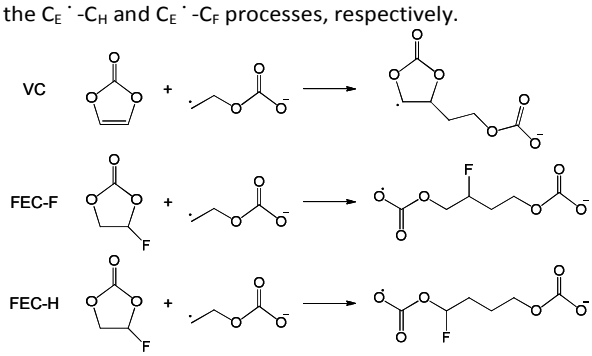

Scheme 1 Reaction between VC and o_E-EC$^-$, and between FEC (C_H and C_F) and o_E-EC$^-$.

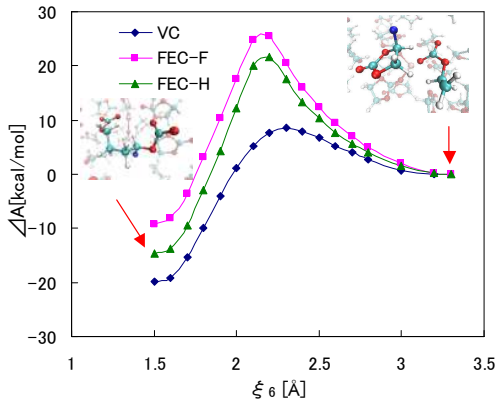

Figure 8 Free energy profiles, ΔA, of the binding reactions between neutral FEC and the o_E-EC$^-$ anion radical along the mechanical constraint, ξ_6, of the distance between the target atom in FEC and the $C_E^{\cdot}$ in o_E-EC$^-$. As denoted in Scheme 1, the labels FEC-H and FEC-F indicate that the attacked atoms in FEC are C_H ($C_E^{\cdot}$-C_H) and C_F ($C_E^{\cdot}$–C_F), respectively. The profile of the reaction between o_E-EC$^-$ and VC is also depicted for comparison.

Compared with the VC case, FEC needs notably larger activation energy to proceed the binding reaction with o_E-EC$^-$. This reactivity difference between FEC and VC is likely to be main chemical difference between these two additives in LIB.

Although the binding reaction between C_C (carbonyl carbon) atom in FEC and $C_E^{\cdot}$ in o_E-EC$^-$ occurred when the reaction sites were close together, the average energy of the trajectory of the product state was higher than that of the reaction state by about 10.6 kcal/mol. Therefore, the o_E-EC$^-$ attack on the C_C atom of FEC was an endothermic reaction, and we conclude that this reaction does not proceed in EC solvent.

To investigate the reactivity of the d_F-FEC neutral radical toward the neutral EC and FEC molecules, we located the C_C atom of d_F-FEC close to a C_E atom of EC or C_F atom of FEC molecule, respectively, and carried out several DFT-MD runs. We found that spontaneous separations of the reactants occur in all the calculations. We also estimated the free energy profile of the binding reaction between the reactive C_c of d_F-FEC and C_F in intact FEC by using the blue-moon ensemble method, and found that the activation free energy was about 40kcal/mol and the reaction free energy was 20kcal/mol, corresponding to endothermic reaction. The details are shown in Supporting Information (ESI). Therefore, we conclude that the d_F-FEC neutral radical is inert to the intact EC and FEC molecules in the solvent. This fact suggests that the contribution of d_F-FEC to the decrease of initial irreversible capacity is smaller than that of the intact VC additive[39]. If the d_F-FEC radical reacts with another d_F-FEC before decomposition, they will react without activation energy and form the oligomer products, which can be related to the observed polymerized-materials in the presence of FEC. Because these oligomer products do not have a C=C double bond, they do not seem to undergo further polymerization the way that the reaction products of VCs do[40]. Furthermore, owing to the absence of Li^+ ions, which act as "glue" in organic SEIs[40], under the environment with the neutral d_F-FEC molecules and their oligomers, organic SFC aggregates formed from the d_F-FEC oligomers are expected to be fragile. This probable fragility can be related to the increase of the irreversible loss of capacity at high FEC concentrations[50]; this loss of capacity is supposed to be caused by the SEI film breakdown during Li^+ ion insertion, because the d_F-FEC oligomer is probably generated predominantly at high FEC concentrations. In contrast, if decomposition of d_F-FEC predominates, the polymerized organic SFCs will not be generated from FEC alone.

In summary, the reactivity of a neutral FEC molecule with an EC anion radical is low compared to neutral VC, and it is likely to be main difference between FEC and VC.

4 Effects of LiF in SEI

4.1 LiF molecules in Li_2EDC aggregate

The results described so far indicate that LiF formation plays a major role in the effects of the FEC additive to the EC solvent. Here we examine the effect of the LiF component on the SEI film associated with the EC solvent molecules. We first carried out DFT-MD calculations to prepare equilibrium trajectories of

aggregate structures of Li_2EDC molecules, and constructed the following two models; (1) LiF molecules distributed in a Li_2EDC aggregate and (2) a LiF aggregate interfaced with a Li_2EDC aggregate. For the former model, we added 5, 10 and 20 LiF molecules in the several snapshots of the equilibrium trajectory of amorphous Li_2EDC as the initial structure, and carried out DFT-MD sampling. By comparing multiple samplings, we determined the equilibrium trajectory for each case.

Figure 9 shows a representative snapshot in the equilibrium trajectory (Fig.9a) and a plot of coordination numbers (CNs) with respect to the distance from the F atom to Li atom in the 10 LiF case as an example (Fig.9b). In Fig.9b we also show the CNs from each Li atom to O_2 and O_1 of Li_2EDC, respectively, with (without) LiF. All the F atoms in the LiF molecules were coordinated by only Li^+ ions no matter how many LiF molecules were added. The average nearest-neighbor CNs from F to Li were estimated to be 3.3, 3.3, and 3.5 for the cases in which 5, 10, and 20 LiF molecules were added, respectively. Each F atom was connected to more than two Li^+ ions originating from Li_2EDC in addition to the intramolecular Li of LiF. These coordinating Li^+ ions were equivalently connected to the F atom with an average length of 1.86 Å, which is larger than the intramolecular bond distance of a LiF molecule (1.56 Å).

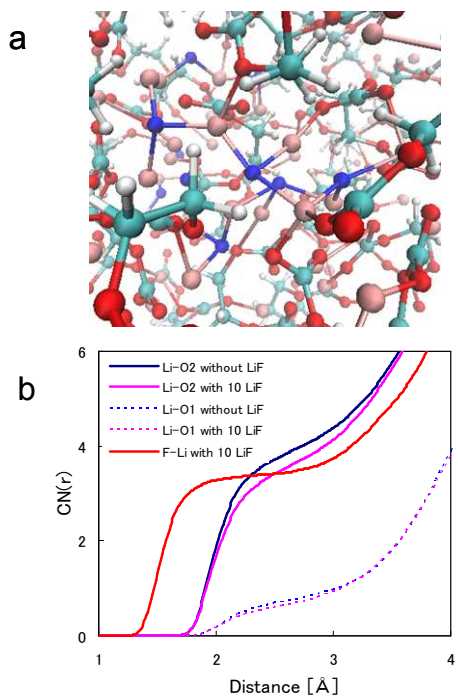

Figure 9 (a) Snapshot of the equilibrium structure around the F atom in a Li_2EDC aggregate containing LiF. Blue, pink, red, cyan, white spheres denote F, Li, O, C, and H atoms, respectively. (b) Red line denotes the Coordination numbers (CNs) from each F atom to the Li^+ ions in the system with 10 LiF molecules in 40 Li_2EDC. Blue (Pink) solid and dashed lines denote CNs from each Li atom to O_2 and O_1 of Li_2EDC, respectively, with (without) 10 LiF in 40 Li_2EDC molecules.

These results indicate that each F atom works as a joint of multiple connections with the Li_2EDC molecules. In the absence of LiF, the Li_2EDC aggregates form a component network via Li-O_1 and Li-O_2 binding[40]. In contrast, the addition of LiF molecules to the Li_2EDC aggregate caused decrease of Li-O_2 bonding and preferential formation of Li-F bonding (See Fig. 9(b)), suggesting that Li-F bonding is stronger than Li-O_2 bonding. Therefore, the mixture of LiF molecules can be expected to change the network in the SFC aggregates and possibly increase the mechanical strength of the SEI film. Recently, Xu et al[51] found that the addition of FEC decreases the number of cracks in a Si nanoparticles electrode after charge-discharge cycles, and concluded that a stable SEI made from FEC limits the formation of the cracks. Their observation seems consistent with our results indicating that LiF in a Li_2EDC aggregate, which is a probable organic component of the SEI films that form in EC electrolytes, stabilizes the SFC aggregate by means of strong F-Li bondings. Our results also suggest that the presence of LiF in the SEI film may suppress Li-ion transport, because the F moieties can act as Li-ion traps. In fact, a decrease in ionic conductivity in the presence of fluorine compounds derived from $LiPF_6$ has been reported[22,23]. Therefore, there will be a LiF concentration in the SEI film that is optimum for better performance.

Regarding the LiF effect on the electric properties, we compared the band gaps of the systems with 5, 10, and 20 LiF molecules in the amorphous Li_2EDC (40 molecules). We randomly chose seven configurations from the equilibrium trajectory of each system. The average band gaps were 4.0, 4.1 and 4.0, respectively. LiF had no observable effect on the band gap in these systems, because the partial density of state (DOS) of Li (F) are located above (below) the conduction (valence) band bottom (top). Therefore, the insulating properties of the aggregates are not affected by the mixture of LiF molecules in the SEI film. The details of the partial DOSs are provided in Supporting Information.

4.2 Interface structure between LiF and Li_2EDC aggregates

To investigate the influence of the interface structure between LiF and the organic SFC aggregates, we constructed an interface between LiF and Li_2EDC aggregates in the EC solvent and estimated the adsorption energy of the Li_2EDC aggregate to the LiF aggregate. Experimental evidence suggests that the inorganic components like LiF and Li_2CO_3 are present in the SEI film[19-21] and that they form interface structures together with the organic components of the SEI. By using the DFT-MD method, we constructed the equilibrium structure of the interface between the LiF and Li_2EDC aggregates; a snapshot of the equilibrium interface structure and a plot of CNs from interfacial Li atoms in the Li_2EDC layer to F atoms in LiF (blue line), O atoms of Li_2EDC (red line), and Li atoms in LiF (gray line) are shown in Fig. 10 a and b, respectively. The Li^+ ions of Li_2EDC aggregate form bonding to the F atoms of LiF aggregate near the interface and to the O atoms of EDC molecules. This equilibrium structure suggests strong adhesion via -F-Li-O- bridging bond between the LiF and Li_2EDC aggregates. Then, we calculated the adhesion energy of the Li_2EDC aggregate to the LiF aggregate in the EC electrolyte. We compared the average total energies of the DFT-MD trajectories where the Li_2EDC aggregate adhered to the LiF aggregate and dissolved into the EC electrolyte.

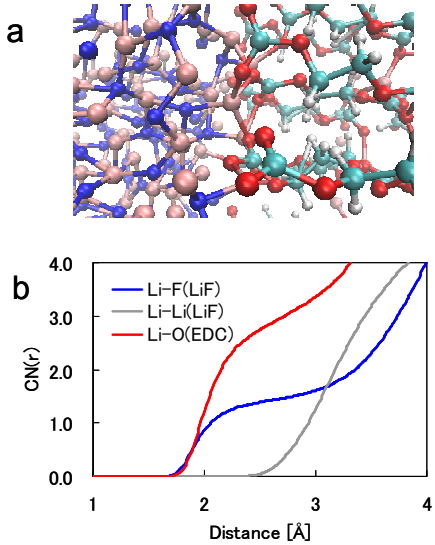

Figure 10 (a): Snapshot of equilibrium structure of the interface between the LiF and Li_2EDC layers. Blue, pink, red, cyan, white spheres denote F, Li, O, C, and H atoms, respectively. The F-Li-O bridge structure between EDC and LiF can be seen. (b) The coordination number (CN) of the interfacial Li^+ ion in Li_2EDC to F atoms (blue), Li atoms in the LiF layer (gray), and O atoms in the Li_2EDC layer (red).

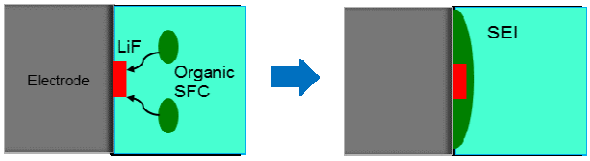

Figure 11 Schematic picture of SEI formation by adsorption of organic SFC aggregates to the LiF components, rather than directly to the electrode.

The estimated adsorption energy was -5.2 kcal/mol (per Li_2EDC molecule), indicating that the Li_2EDC aggregate preferred to adhere to the LiF aggregate. This result is in contrast to the results for a graphite edge H-capped surface, where the Li_2EDC aggregate shows no tendency to adhere. This adhesion of Li_2EDC can be associated with the stability of the organic SFC molecules around the electrodes.

The high electron affinity of FEC facilitates generation of LiF molecules preferentially via the FEC reductive decomposition, and LiF aggregates are expected to appear on the anode surface. Organic SFC molecules like Li_2EDC will adhere to the surface of LiF aggregates by F-Li bonding, as suggested above, and will form the stable organic part of SEI film on the anode where the Li^+ ions can easily penetrate. In fact, recent X-ray photoelectron spectroscopy (XPS) measurements[21.] clearly indicate that LiF and Li_2CO_3 are plentiful on a graphite electrode surface. However, it is also reported that distinction between graphite and C-C/C-H bonds is reported to be subtle in the XPS images, and imaging indicates that there are many microscopic pores for the organic components between the inorganic species. In Fig. 11, we show a schematic picture of our view of adsorption of organic SFC to the electrode with help of LiF aggregate. The preferential adsorption of organic SFC aggregates to LiF surface rather than the electrode surface can be expected to contribute to development of a stable passivating SEI film. In addition, the stabilization of the SEI film may be related to the decrease of capacity fading due to FEC in the case of a silicon anode. The rapid volume change of silicon anode during charge-discharge process likely induces desorption of organic SFC aggregate from its surface. Therefore, stability of SEI film is effective for the decrease of capacity fade.

4.3 Interface structure between LiF aggregate and lithiated silicon anode

Then, we investigated the structure of the interface between a LiF aggregate and a silicon anode (a LiSi/LiF/EC system), and compared the interface structure with that for a graphite edge H-capped surface (a graphite/LiF/EC system). We modeled the lithiated silicon anode with a $Li_{64}Si_{64}$ alloy and calculated the equilibrium structure of LiF aggregate adsorption to the silicon anode in EC electrolyte modeled with 64 EC molecules. We show the representative equilibrium structures of the lithiated silicon anode and H-capped graphite anode with the LiF aggregate in an EC electrolyte in Fig.12. We can see the formation of bonds between the Li in the lithiated silicon and the F in the LiF aggregate in Fig.12a. The average F-Li bond length was about 1.78 Å. These bonds suggest that the LiF aggregate stably adsorbed to the lithiated silicon anode, and the adsorbed LiF aggregate probably acts as a glue for organic SFC molecules, as mentioned above. Comparison between snapshots of the initial and equilibrium states of the LiSi/LiF/EC system (see Figure S12 in Supporting Information) clearly indicates formation of bonding between the LiF aggregate and the lithiated silicon anode. In contrast, on the H-capped graphite anode, no bonds formed between the anode and the LiF aggregate, as expected (Fig12.b).

In fact, the average energy of the adhesion state of LiF aggregate to the H-capped graphite anode was 18.7 kcal/mol higher than that of the state in which the LiF aggregate was dissolved in the EC electrolyte. This result indicates that Si anode can form a stable LiF layer on the surface by means of strong Li-F bondings, different from the H-capped graphite anode. Therefore, FEC is more effective as a stable glue for organic SFCs on the Si anode. This further enables quicker completion of the SEI film formation and thus inhibition of further reduction of the electrolyte. This suggests that the thickness of the organic SFC aggregate can be thinner in the presence of LiF and thus FEC, which was actually observed in experiments[11.,45.]. Detailed results of the DFT-MD run for the LiSi/LiF/EC system are given in Supporting Information.

Here we comment on the LiF produced by decomposition of PF_6^- anion. It is well known that LiF is also generated by the reductive decomposition of PF_6^- anion. As the recent study by Takenaka et al[28.] pointed out, it is difficult for PF_6^- anion to get closer to the negatively charged electrode and the amount of LiF generated in the presence of PF_6^- is small compared to the amount generated in the presence of FEC addition. Thus, the ability of FEC to diffuse close to the electrode surface may be related to the effectiveness of LiF in the SEI film.

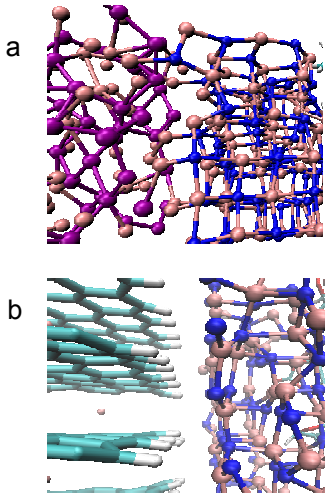

Figure 12 Snapshots of the equilibrium structures of a LiF aggregate interfaced with (a) a lithiated silicon anode, and (b) a H-capped graphite anode, respectively. Blue, pink, purple, cyan, white spheres denote F, Li, Si, C, and H atoms, respectively.

Finally, we emphasize the difference between the effects of the VC and FEC additives on SEI film formation. VC is characterized by its reactivity to anion radicals in its neutral state as our previous studies demonstrated, and the effects of added VC, such as the decrease in irreversible capacity, are attributed to its reaction process. In contrast, the main role of FEC is the generation of LiF, which may contribute to the adhesion or aggregation properties of SFCs. Thus, the present results demonstrate that the effects of additives can differ even if their structures and chemical formulas are similar. Note that the role of the additive also depends on the nature of the electrode surface.

5 Conclusions

By using DFT-MD sampling and the blue-moon ensemble technique to investigate free energy changes, we investigated various pathways for reductive decomposition of FEC and elucidated the most plausible reductive process. Via cleavage of the C_C-O_F "shoulder" bond, FEC generated LiF with almost no activation barrier, whereas the cleavage of the "waist" bonds, C_H-H_H and C_F-H_F, of FEC resulted in a large gain in reaction energy, but the activation energy of the reaction was higher than that for C_C-O_F bond cleavage. Furthermore, electron transfer to the EC solvent frequently occurred before the bond was broken. Therefore, the cleavage of the C_H-H_H and C_F-H_F bonds by one electron reduction does not predominate in the EC solvent. On the basis of the present calculations, we confirmed that FEC in the EC electrolyte exerts its effects mainly via the generation of LiF, as the previous computational studies have suggested[52]. The $C_3H_3O_3$ neutral radical produced by the LiF release is inert to neutral molecules, EC and FEC, and decomposes to generate CO_2 gas if it does not react with other radical molecules. Furthermore, the reaction of a neutral FEC molecule with an EC anion radical requires a larger activation energy than in the VC additive case, and this difference leads to a substantial difference between FEC and VC.

To evaluate the effects of the LiF released from FEC, we investigated the LiF state in an organic SFC (Li_2EDC) aggregate, and the adhesion properties of an amorphous LiF aggregate to the organic SFCs as well as to a model Si anode. LiF molecules in the Li_2EDC aggregates show that the Li-F bond was elongated and the F atom was coordinated by approximately three Li atoms in the Li_2EDC aggregates. The F atoms connected the Li atoms in the Li_2EDC aggregate by strong Li-F bonding. Therefore, the LiF in Li_2EDC aggregates can be expected to efficiently stabilize the SEI. We also investigated the effect of the interface between LiF and Li_2EDC aggregates. The Li atom in the Li_2EDC aggregate bonded strongly to the F atom in the LiF aggregate. This bonding between Li and F around the interface suggests strong adhesion between the LiF and the organic components in the SEI. In fact, the estimated energy of adhesion of the Li_2EDC aggregate to the LiF aggregate shows the stability of the adsorbed state of Li_2EDC to the LiF layer in the EC electrolyte. This adhesion may also explain the stability of the SEI film formed from FEC, and LiF is likely to act as a glue to organic SFC like Li_2EDC in LIBs. Finally, we examined the interface structure of the LiF aggregate to a lithiated silicon anode and compared the structures with that of the interface between LiF and a pristine H-capped graphite anode. The formation of a bond between Li in the anode and F in the LiF aggregate was observed in the case of the lithiated silicon anode, whereas no bonding was observed in the graphite case. This result suggests that FEC is more effective for use with Si anode than that with graphite anode.

Acknowledgements

Y.O and K. U. acknowledge Dr. H. Watanabe and Dr. K. Furuya of FUJIFILM Corp. for their support. This work was supported by KAKENHI 23340089 as well as by the Strategic Programs for Innovative Research (SPIRE), MEXT and the Computational Materials Science Initiative (CMSI), Japan. The calculations in this work were carried out at the super-computer centers of NIMS and the University of Tokyo, as well as on the K computer at the RIKEN AICS through the HPCI System Research Projects (Proposal Numbers hp140071 and hp140232)

Notes and references

1. W.Kohs, H.J.Santner, F.Hofer, H. Schrottner, J. Doninger, I.Barsukov, H.Buqa, J.H.Albering, K.C. Moller,J.O.Besenhard, and M. Winter, *J. Power Sources* 2003, **119**, 528-537.
2. R. Fong and U.von Sacken,J.R.Dahn Studies, *J. Electrochem. Soc.* 1990, **137**, 2009-2013.
3. T.R.Job, K.Xu,O.Borodin,and M.Ue, *Electrolytes for Lithium and Lithium-Ion Batteries (Modern Aspects of Electrochemistry)*;, Eds. Springer-Berlin, 2014.
4. Y. Wang andP.B.Balbuena, Eds. *Lithium-Ion Batteries: Solid-Electrolyte Interphase*; Imperial College:London, 2004.
5. P.Verma, P.Maire, and P.Novák, *Electrochimica Acta* 2010, **55**, 6332-6341.
6. M.Nie, D.Chalasani, D.P.Abraham, Y.Chen, A.Bose, and B.L. Lucht, *J. Phys. Chem. C.* 2013, **117**, 1257-1267.
7. D. Aurbach, E.Zinigrad, Y.Cohen, and H. Teller, *Solid State Ionics* 2002, **148**, 405-416.

8. J.Vetter, P.Novák, M.R.Wagner,C.Veit, K.-C.Möller, J.O.Besenhard, M.Winter, M.Wohlfahrt-Mehrens,C.Vogler, and A. Hammouche, *J. Power Sources* 2005, **147**, 269-281.
9. S. Leroy, F. Blanchard, R.Dedryvère, H.Martinez, B.Carré, D.Lemordant,and D.Gonbeau, *Surf. Interface Anal.* 2005, **37**, 773-781.
10. D. Aurbach,K. Gamolsky, B.Markovsky, Y.Gofer, M. Schmidt, and U.Heider, *Electrochimca Acta* 2002, **47**, 1423-1439.
11. S.-K.Jeong, M.Inaba, R.Mogi, Y.Iriyama, T.Abe, and Z. Ogumi, *Langmuir* 2001, **17**, 8281-8286.
12. S.-K.Jeong, M.Inaba, T.Abe, and Z.Ogumi, Surface *J. Electrochem. Soc.* 2001, **148**, A989-A993.
13. J.C.Burns, R.Petibon, K.J.Nelson, N.N. Sinha, A.Kassam, B.M.Way,and J.R.Dahn, *J. Electrochem. Soc.* 2013, **160**, A1668-A1674.
14. S.S.Zhang, *J. Power Sources* 2006, **162**, 1379-1394.
15. V.A.Agubra and J.W.Fergus, *J. Power Sources*, 2014, **268**, 153-162.
16. A.M.Andersson, A.Henningson, H.Siegbahn, U.Jansson, and K. Edström, *J. Power Sources*. 2003, **119-121**, 522-527.
17. H.Ota, Y.Sakata, A.Inoue, and S.Yamaguchi, *J. Electrochem. Soc.* 2004, **10**, A1659-A1669.
18. H.L. Huang, Z.H.Min, and Q.Y.Zhang, *Rev. Adv. Mater. Sci.* 2014, **36**, 13-20.
19. K.Edström, M.Herstedt, and D.P.Abraham, *J. Power Sources* 2006, **153**, 380-384.
20. E.Peled, D.Golodnitsky,and G.Ardel, *J. Electrochem. Soc.* 1997, **144**, L208-L210
21. P.Niehoff,S.Passerini,and M.Winter, *Langmuir*, 2013, **29**, 5806
22. D.Aurbach, K.Gamolsky, B.Markovsky,G.Salitra,Y.Gofer, U. Heider, R. Oesten, and M.Schmidt, *J. Electrochem. Soc.* 2000, **147**, 1322-1331
23. D.H.Jang and S.M.Oh, *J. Electrochem.Soc.* 1997, **144**, 3342-3348
24. K.Tasaki, *J. Phys. Chem. B* 2005, **109**, 2920-2933.
25. O.Borodin,G.D.Smith, and P.Fan, *J. Phys. Chem. B* 2006, **110**, 22773-22779.
26. O.Borodin, G.V.Zhuang, P.N.Ross, and K.Xu, *J. Phys. Chem. B* 2013, **117**, 7433-7444
27. N.Takenaka, Y.Suzuki, H.Sakai, and M.Nagaoka, *J. Phys. Chem. C* 2014, **118**, 10874-10882.
28. N.Takenaka, H.Sakai, Y.Suzuki, P.Uppula, and M.Nagaoka, *J. Phys. Chem. C* 2015, **119**, 18046-18055.
29. A. Marquez, *Mater. Chem. Phys.* 2007, **104**, 199-209.
30. Y.-K.Han,S.U.Lee, J.H.Ok, J.J.Cho, and H.J.Kim, *Chem. Phys. Lett.* 2002, **360**, 359-366.
31. S.Matsuoka, T.Asada,and K.Kitaura, *J. Electrochem. Soc*. 2000, **147**, 1695-1702.
32. Y.Wang and P.B.Balbuena, *J. Phys. Chem. A* 2002, **106**, 9582-9594.
33. Y.Wang, S.Nakamura, M.Ue, and P.B.Balbuena, *J. Am. Chem. Soc.* 2001, **123**, 11708-11718.
34. Y.Wang, S.Nakamura, K.Tasaki, and P.B.Balbuena, *J. Am. Chem. Soc.* 2002, **124**, 4408-4421.
35. K.Leung and J.L.Budzien, *Phys. Chem. Chem. Phys.* 2010, **12**, 6583-6586.
36. K.Leung, *Phys. Chem. Chem. Phys.* 2015, **17**, 1637-1643.
37. S.Ogata, N.Ohba, and T.Kouno, *J. Phys. Chem. C* 2013, **117**, 17960-17968.
38. P.Ganesh, P.R.C.Kent, and D.-e.Jiang, *J. Phys. Chem. C* 2012, **116**, 24476-24481.
39. K.Ushirogata, K.Sodeyama, Y.Okuno, and Y.Tateyama, *J. Am.Chem. Soc.* 2013, **135**, 11967-11974.
40. K.Ushirogata, K.Sodeyama, Z.Futera, Y.Tateyama, and Y. Okuno, *J. Electrochem. Soc.* 2015, **162**, A2670-A2678.
41. N.S.Choi, K.H.Yew, K.Y.Lee, M.Sung, H.Kim, and S.S.Kim, *J. Power.Sorce.* 2006, **161**, 1254-1259
42. V.Etacheri, O.Haik, Y.Goffer, G.A.Roberts, L.C.Stefan, and R.Fasching, D.Aurbach, *Langmuir*, 2011, **28**, 965-976
43. R.Elazari, G.Salitra, G.Gershinsky, A.Garsuch, A.Panchenko, A, and D.Aurbach, *J.Electrochem.Soc*. 2012, **159**, A1440-A1445
44. S.Dalavi, P.Guduru, and B.L. Lucht, *J. Electrochem.Soc*. 2012, **159**, A642-A646.
45. H.Nakai, T.Kubota, A.Kita, and A.Kawashima, *J. Electrochem.Soc.* 2011, **158**, A798-A801.
46. I.A.Profatilova, C.Stock, A.Schmitz, S.Passerini, and M.Winter, *J.Power. Sources*. 2013, **222**, 140-149.
47. I.A.Profatilova, S.S.Kim, and N.S.Choi, *Electrochimica Acta*. 2009, **54**, 4445-4450
48. S.Komaba, T.Ishikawa, N.Yabuuchi, W.Murata, A.Ito, and Y.Ohsawa, *Appl.Mat.Interfaces.* 2011, **3**, 4165-4168
49. L.Chen, K.Wang, X.Xie, and J.Xie, *J.Power.Sorce.* 2007, **174**, 538-543
50. X.Zhao, Q.C.Zhuang, S.D.Xu, Y.X.Xu, Y.L.Shi, X.X.Zhang, *Int.J.Electrochem.Sci.* 2015, **10**, 2515-2534
51. C.Xu, F.Lindgren, B.Philippe, M.Gorgoi, F.Bjorefors, K.Edstrom, T.Gustafsson, *Chem.Mat.* 2015, **27**, 2591-2599
52. K.Leung, S.B.Rempe, M.E.Foster, Y.Ma, J.M.Martinez, D.L.Hoz, N.Sai, and P.B.Balbuena *J. Electro.Chem.Soc.* 2014, **161**, A213-A221
53. Y.Ma and P.B.Balbuena, *J. Electro.Chem.Soc.* 2014, **161**, E3097-E3109
54. D.L.H.Martinez and P.B.Balbuena, *Phys. Chem. Chem. Phys.* 2014, **16**, 17091-17098.
55. R. Car and M.Parrinello, *Phys. Rev. Lett.* 1985, **55**, 2471-2474.
56. CPMD, http://www.cpmd.org/, Copyright IBM Corp 1990-2008, Copyright MPI für Festkörperforschung Stuttgart 1997-2001.
57. S.Nose *J. Chem. Phys.* 1984, **81**, 511-519.
58. W.G.Hoover, *Phys. Rev. A*, 1985, **31**, 1695-1697.
59. M.Sprik and G.Ciccotti, *J. Chem Phys.* 1998, **109**, 7737-7744
60. J.P.Perdew, K.Burke, and M.Ernzerhof, *Phys. Rev. Lett.* 1996, **77**, 3865-3868.
61. J.P.Perdew, K.Burke, and M.Ernzerhof, *Phys. Rev. Lett.* 1997, **78**, 1396.
62. S.Goedecker, M.Teter, and J.Hutter, *Phys. Rev. B* 1996, **54**, 1703-1710.
63. C.Hartwigsen, S.Goedecker, and J.Hutter, *Phys. Rev. B* 1998, **56**, 3641-3662.

64. M.Krack, *Theor. Chem. Acc.* 2005, **114**, 145-152.
65. A.D.Becke, *J.Chem.Phys.* 1993, **98**, 1372-1377
66. M.J.Frisch,G.W.Trucks, H.B.Schlegel, G.E.Scuseria, M.A.Robb, J.R.Cheeseman, G.Scalmani, V.Barone, B.Mennucci, G.A.Petersson, *et al.* Gaussian 09, Revision D.01; Gaussian, Inc., Wallingford CT, 2009.